# RECENT DEVELOPMENT IN HIGH -TEMPERATURE PERMANENT MAGNET MATERIALS

**Abstract**--Future advanced power systems require permanent magnets capable of operating at temperatures higher than 400°C. The best conventional high-temperature permanent magnets can operate reliably up to 300°C. One important factor that limits the conventional permanent magnets for operation at temperatures higher than 300°C is the low intrinsic coercivity ($_MH_c$) at high temperatures, which results in non-linear induction demagnetization curve (B curve) and makes the magnets unsuitable for dynamic applications, for example, for motors and generators.

Systematic studies have been carried out in $Sm(Co_{1-v-x-y}Fe_vCu_xZr_y)_z$ with v = 0 to 0.3, x = 0 to 0.2, y = 0 to 0.06, and effective z = 7.0 to 8.2. It was observed that high-temperature performance of sintered $Sm(Co_{1-v-x-y}Fe_vCu_xM_y)_z$ magnets is very sensitive to the Fe and Sm contents in the magnet alloys. Generally speaking, magnets containing lower Fe and higher Sm displayed higher intrinsic coercivity at high temperatures. Based on these studies, new sintered high-temperature permanent magnet materials have been successfully developed and the highest operating temperature of permanent magnets has been increased to 550°C. These new magnets demonstrate excellent long-term stability and superior dynamic magnetic properties at high temperatures. These advances represent a breakthrough in high-temperature permanent magnets research and development.

## 1. Introduction

### 1.1 Requirement for high-temperature permanent magnet materials

Permanent magnet materials capable of reliably operating at high temperatures (≥400°C) are required for future advanced power systems in a proposed More Electric Aircraft (MEA) initiative. A major objective of the MEA initiative is to increase aircraft reliability, maintainability, and supportability, including drastically reducing the need for ground support equipment. This advancement will be accomplished in part through the development of advanced power components such as magnetic bearings, Integrated Power Units, and Internal Starter/Generators for main propulsion engines. New high temperature magnets are enabling technologies for the development of these new power components. Power system designers frequently find that magnetic materials impose technological limitations on their designs. Compromises are generally required between the desired performance and the magnetic, mechanical, and electrical properties of available materials. If new materials can operate at ≥ 400°C, then new advanced designs will be possible. Air-cooling, rather than complicated liquid cooling and its necessary logistic support, will become an operational capability. Likewise, oilless/lubeless gas turbine engines and space power systems will be possible.

### 1.2 Review of conventional permanent magnet materials

Currently, the most widely used permanent magnet materials are Alnico, hard ferrites, and high-performance rare earth-transition metal (RE-TM) permanent magnets, including $SmCo_5$, $Sm_2(Ce,Fe,Cu,Zr)_{17}$ ($Sm_2TM_{17}$ or 2:17), and Nd-Fe-B magnets. Figures 1-1 and 1-2 summarize temperature dependence of the maximum energy product, $(BH)_{max}$, and intrinsic coercivity, ${}_MH_c$, for five types of commercial permanent magnetic materials [1]. As shown in these figures, the magnetic properties of rare earth magnets are superior to all other magnet materials. Among rare earth magnets, Nd-Fe-B-type magnets have the highest static $(BH)_{max}$ at temperatures $T < 130°C$. At $T > 130°C$, $Sm_2TM_{17}$ (2:17) magnets have the highest $(BH)_{max}$. The only magnet that maintains relatively high intrinsic coercivity (~10 kOe) at high temperature up to 300°C is $Sm_2TM_{17}$.

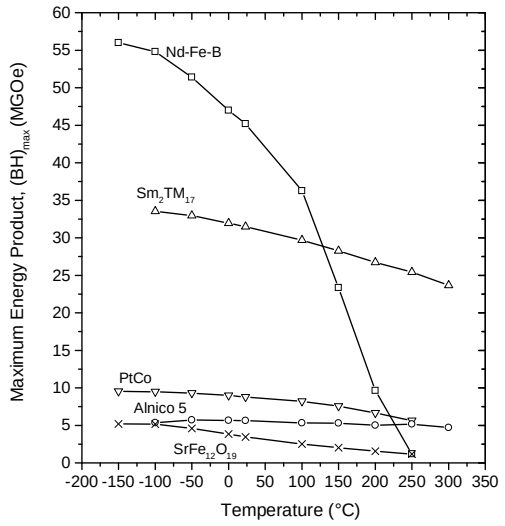


Figure 1.1. Temperature dependence of $(BH)_{max}$ for five types of permanent magnets.

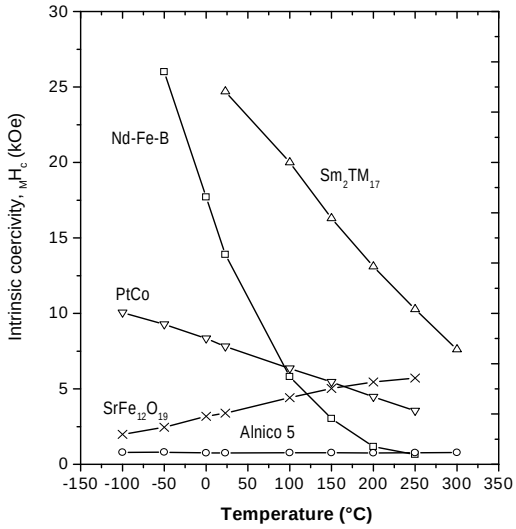


Figure 1.2. Temperature dependence of ${}_MH_c$ for five types of permanent magnets.

The best conventional high-temperature 2:17 magnets can operate up to 300°C. The problem associated with higher temperature (> 300°C) operation has been that the intrinsic coercivity of these magnets drops sharply with increasing temperature. Upon heating, ${}_MH_c$ of the 2:17 magnets drops sharply from their room temperature values of 20 to 30 kOe (or higher) to only 3 to 6 kOe at 400°C and 1 to 3 kOe at 500°C (Figure 1-3). Low intrinsic coercivity at high temperatures results in nonlinear 2nd-quadrant induction demagnetization curves (B curves) above ≈ 300ºC. A linear 2nd-quadrant B curve is critical for all dynamic applications, such as for generators and motors.

In a dynamic application, the operating point of a magnet keeps cycling. If the intrinsic coercivity is low, then the induction demagnetization curve can be nonlinear. Under this circumstance, the operating point of the magnet can be reduced to below the knee in the induction demagnetization curve and the induction can be significantly reduced irreversibly. If the intrinsic coercivity of the magnet is sufficiently high, then the induction demagnetization curve can be linear. Under this circumstance, the induction will be reversible around the operating point even at a quite low permeance value as shown in Figure 1-4. The maximum operating temperature of a magnet can be defined as the temperature limit at which the induction demagnetization curve of the magnet still maintains the linearity. Therefore, in

order to increase the operating temperature of permanent magnet materials, the key is to increase intrinsic coercivity at high temperature, so that their induction demagnetization curves remain linear at the operating temperature.

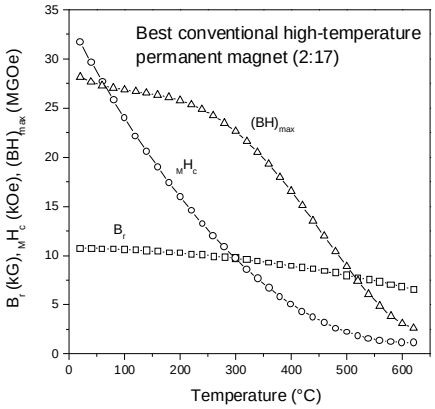


Figure 1-3. Temperature dependence of the best conventional high-temperature 2:17 magnet.

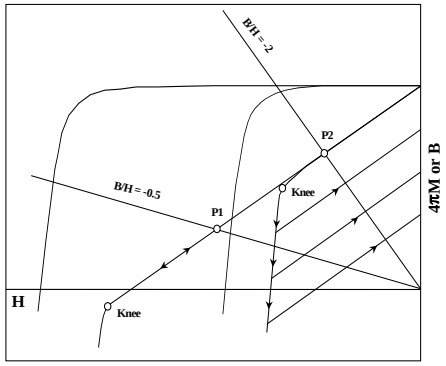


Figure 1-4. Intrinsic coercivity and linearality of induction demagnetizaiton curve.

**2. Candidate alloy system for high –temperature permanent magnet materials**

The two criteria of high-temperature permanent magnets are high Curie temperature and high magneto-crystalline anisotropy. At least within the foreseeable future, these requirements can be met probably only in Sm-Co based system. It is well known that in a rare earth-transition metal (RE-TM) compound, the Curie temperature is primarily determined by the TM sublattice, while the crystalline anisotropy is primarily contributed by the RE sublattice unless at temperature as high as close to Curie point. Research on RE-TM compounds has indicated that among all TM, Co provides the highest Curie temperature, while among all light rare earths, Sm usually provides the highest crystalline anisotropy.

Figure 2-1 shows Curie temperature, $T_C$, versus Co content in Sm-Co binary compounds. In this figure, Curie temperature data for $LaCo_{13}$ and $Sm_2Co_{14}B$ are also included. It can be seen from Figure 2-1 that there exists a almost linear relationship between the Curie temperature and the Co content: the higher the Co content in a compound, the higher the Curie temperature of the compound, which clearly demonstrates the importance of the Co content to the Curie temperature. Figure 2-2 illustrates anisotropy field, $H_A$, in binary $RECo_5$ compounds with RE = Y, La, Ce, Pr, Nd, Sm, and MM. It is obvious that $SmCo_5$ compound has the highest anisotropy filed. Figure 2-3 shows anisotropy field, $H_A$, in binary $RE_2Co_{17}$ compounds with RE = Y, Ce, Pr, Nd, and Sm. It is of interesting that for 2:17 type of compounds only $Sm_2Co_{17}$ has uniaxial magneto-crystalline anisotropy and, therefore, possesses a large crystalline anisotropy field. Sm even behaviors uniquely in ternary $RE_2Fe_{14}B$ compounds. The magneto-crystalline constant $K_1$ of $Sm_2Fe_{14}B$ is of a negative value as shown in Figure 2-4. This means that the easy magnetization direction for $Sm_2Fe_{14}B$ is in the basal plane rather than along the c-axis, such as in the cases for RE = Y, Ce, Pr, and Nd. However, the absolute value of $K_1$ for $Sm_2Fe_{14}B$ is the largest, which means that there exists the largest magneto-crystalline anisotropy between the basal plan and the c-axis for $Sm_2Fe_{14}B$.

It can be concluded from the above analysis that until a totally new high-temperature permanent magnet material is discovered in future, an appropriate approach to developing better high-temperature permanent magnet materials that

satisfy the requirements of the advanced power devices is to significantly improve the conventional Sm-Co type magnets, especially $Sm_2(Co,Fe,Cu,Zr)_{17}$ magnets and to develop new compounds based on Sm-Co compounds.

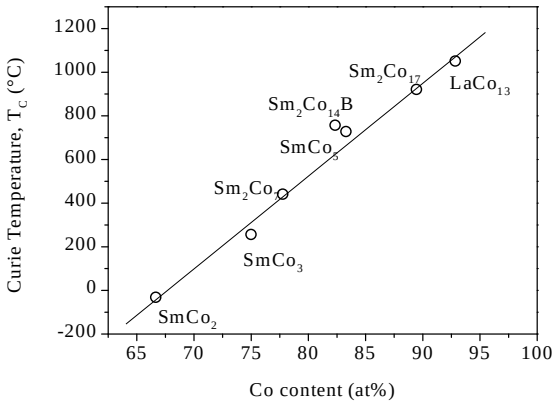


Figure 2-1. Curie temperature, $T_C$, versus Co content in Sm-Co binary compounds. Data for $LaCo_{13}$ and $Sm_2Co_{14}B$ are also included.

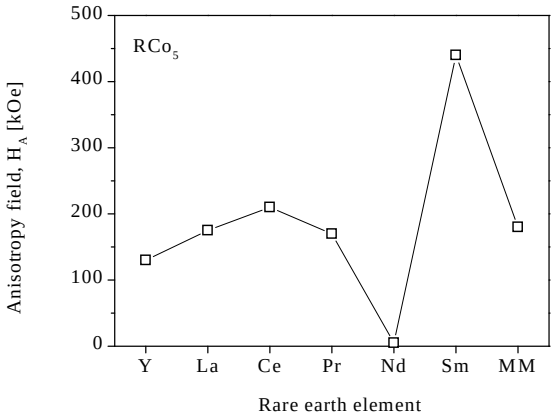


Figure 2-2. Anisotropy field, $H_A$, in binary $RECo_5$ compounds.

effects of compositions on magnetic properties of the 2:17 permanent magnets have been investigated in the past 20 years [1-6]. More recently, the relationship between composition and the high-temperature performance of the 2:17 magnets and alloys have been studied [7-12]. The purpose of this study is to significantly enhance the intrinsic coercivity of $Sm(Co,Fe,Cu,Zr)_z$ permanent magnets based on systematically studies of the effects of composition on high-temperature performance of sintered $Sm(Co,Fe,Cu,Zr)_z$ magnets.

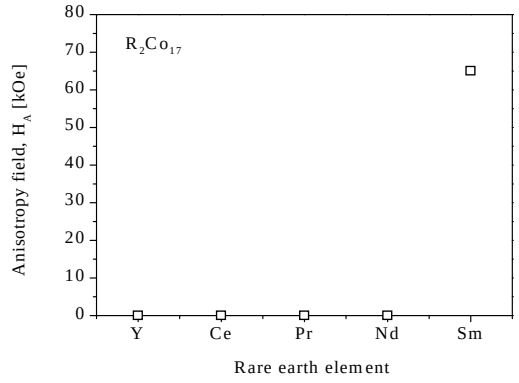


Figure 2-3. Anisotropy field, $H_A$, in binary $RE_2Co_{17}$ compound.

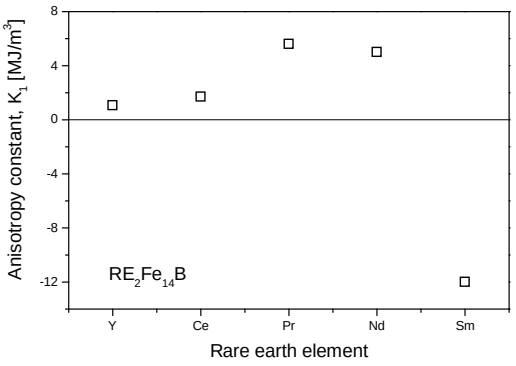


Figure 2-4. Anisotropy constant $K_1$ in $RE_2Fe_{14}B$ ternary compounds

### 3. New $Sm_2Co_{17}$ based high-temperature permanent magnet materials

In recent years extensive research has been carried out to substantially improve the high-temperature performance of the Sm-TM permanent magnets and breakthrough was made in 1999. As a result, the maximum operating temperature of permanent magnets was increased from around 300°C to as high as 550°C. This advance was made on

systematic studies of the effects of compositions on high-temperature intrinsic coercivity of Sm-TM type of permanent magnets.

### 3.1 Effects of compositions on high-temperature intrinsic coercivity of Sm-TM permanent magnets

#### 3.1.1 Effect of Sm on high-temperature intrinsic coercivity of Sm-TM permanent magnets

The Sm content, or the z value in $Sm(Co,Fe,Cu,Zr)_z$, strongly affects the intrinsic coercivity of $Sm_2(Co,Fe,Cu,Zr)_{17}$ type of permanent magnets. As early as in 1982, S. Liu [2] et al. determined the temperature dependence of xx and xx up to 750°C and observed that the magnet specimen that had smaller z value (higher Sm content) possessed higher intrinsic coercivity at high temperatures. A. Kim [3] J.F. Liu [4]

When dealing with the effect of Sm content or z value, it is important to realize that not all Sm exists in Sm-TM compounds in sintered $Sm_2(Co,Fe,Cu,Zr)_{17}$ type of magnets. A small amount of Sm exists in the form of $Sm_2O_3$. This is because Sm is a very active element, some Sm is oxidized during the fine-powder processing and forming Sm oxide. Under a normal condition, a sinter $Sm_2(Co,Fe,Cu,Zr)_{17}$ magnet contains 0.3 – 0.5 wt% oxygen. It is easy to understand that for each 0.1 wt% oxygen there will be 0.627 wt% Sm to be consumed and reacted with oxygen. Therefore, it is useful to define a effective z value which represents the atomic ratio of the transition metals over the metallic part of Sm.

Generally speaking, decreasing the z value (increasing the Sm content) of the conventional 2:17 magnets results in decreased intrinsic coercivity at room temperature, but increased intrinsic coercivity at high temperatures. Figure 3-1 summarizes the effect of z value on ${}_MH_c$ of $Sm(Co_{0.795}Fe_{0.09}Cu_{0.09}Zr_{0.025})_z$. Both effective and nominal z values are give in this figure. The effective z value in most conventional 2:17 magnets is approximately 8.3 - a value much higher than all magnets presented in this figure. It can be seen from Figure 3-1 that ${}_MH_c$ at room temperature is very sensitive to the z value and ${}_MH_c$ increases rapidly with increasing z. As temperature rises, especially when $T \geq 500°C$, ${}_MH_c$ becomes less sensitive to z. It can be seen that there is a peak (denoted by pk) in each ${}_MH_c$-z curve in the temperature range of 300-500°C. It is interesting to note that as temperature increases, the z value corresponding to the peak ${}_MH_c$ shifts toward lower values of z. As shown in Fig. 3.2, the effective z values corresponding to the peak ${}_MH_c$ at 300, 450, and 500°C are 7.86, 7.62, and 7.38, respectively. It is obvious that at room temperature the peak should occur at $z \geq 8.10$, while at 550 and 600°C the peaks should occur at $z \leq 7.14$.

It can also be concluded from Figure 3-1 that ${}_MH_c$ becomes more and more sensitive to temperature with increasing z. This trend can be seen more clearly from Figure 3-2, which shows the temperature dependence of ${}_MH_c$ for $Sm(Co_{0.795}Fe_{0.09}Cu_{0.09}Zr_{0.025})_z$. It can be seen from Figure 3-2 that when the effective $z = 7.14$, the coercivity slightly increases with increasing temperature in the temperature range from 300 to 450°C. As z increases, ${}_MH_c$ gradually increases in the temperature ??????.

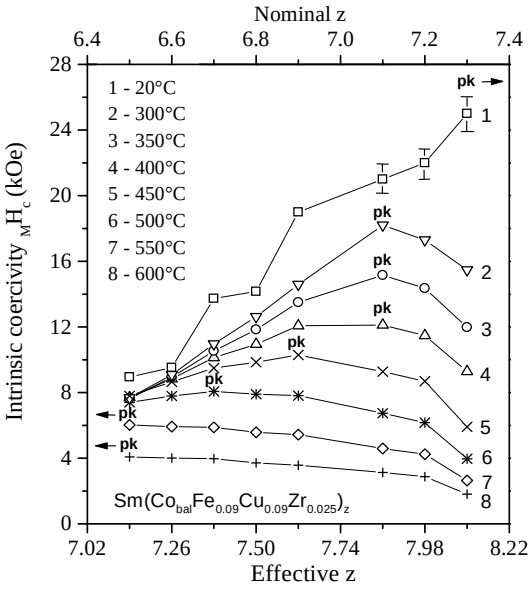


Figure 3-1. Dependence of intrinsic coercivity of $Sm(Co_{0.795}Fe_{0.09}Cu_{0.09}Zr_{0.025})_z$ on z value at various temperatures.

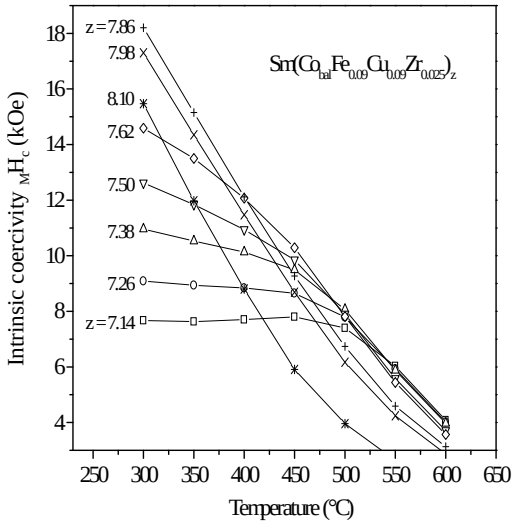


Figure 3-2. Temperature dependence of intrinsic coercivity for $Sm(Co_{0.795}Fe_{0.09}Cu_{0.09}Zr_{0.025})_z$ from 300 to 600°C.

### 3.1.2 Effect of Fe on High Temperature $_MH_c$ of Sm-TM Magnets

Fe also has strong effect on high-temperature coercivity of $Sm_2(Co,Fe,Cu,Zr)_{17}$ type of permanent magnets. Increasing Fe content in 2:17 type magnets effectively enhances their saturation magnetization and maximum energy product. However, it was observed in the middle of 1990s that high Fe content (or low Co content) in the magnets resulted in poor high-temperature stability of the magnets [4-6]. J.F. Liu [7]

Generally speaking, decreasing Fe content (increasing Co content) in the 2:17 magnets does not strongly affect their room temperature coercivity, but significantly enhances their coercivity at high temperatures. Effect of Fe content on intrinsic coercivity in $Sm(Co_{bal}Fe_vCu_{0.09}Zr_{0.03})_{7.5}$ at high temperatures from 400°C to 600°C is given in Figure 3-3. It should be noted that the Fe content in conventional 2:17 magnets is v = 0.21 - 0.31, much higher than the Fe content in magnet materials in this study. It can be seen from Figure 3-3 that the high-temperature $_MH_c$ increases rapidly with decreasing Fe content in the magnet alloys. At 400°C, $_MH_c$ increases from 5.6 kOe when v = 0.22 to 12.7 kOe when v = 0.1. A coercivity peak appears when v = 0.1 at 400°C. This peak shifts to v= 0.07 at higher temperatures.

### 3.1.3. Effect of Cu on High Temperature $_MH_c$ of Sm-TM Magnets

It is well known that coercivity in the $Sm_2(Co,Fe,Cu,Zr)_{17}$ type of magnets originates from the pinning of domain wall in the Cu-rich cell boundary phase in a fine-scaled cellular microstructure. Therefore, sufficient Cu content is essential in order to develop high coercivity at both room temperature and high temperatures. Generally speaking, $_MH_c$ increases with the Cu content monotonously. However, the effect of Cu on increasing $_MH_c$ is quite different at different temperatures. Figure 3-4 shows temperature dependence of intrinsic coercivity for $Sm(Co_{bal}Fe_{0.1}Cu_xZr_{0.025})_{6.7}$. It was observed that when a magnet containing very low Cu, its $_MH_c$ could have a positive temperature coefficient. This abnormal temperature dependence of intrinsic coercivity is explained in Section 3.9.

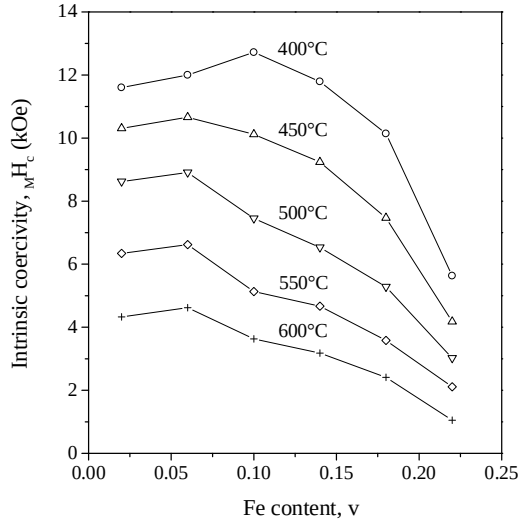


Figure 3-3. High-temperature intrinsic coercivity, $_MH_c$, as a function of Fe content, v, in $Sm(Co_{bal}Fe_vCu_{0.09}Zr_{0.03})_{7.5}$.

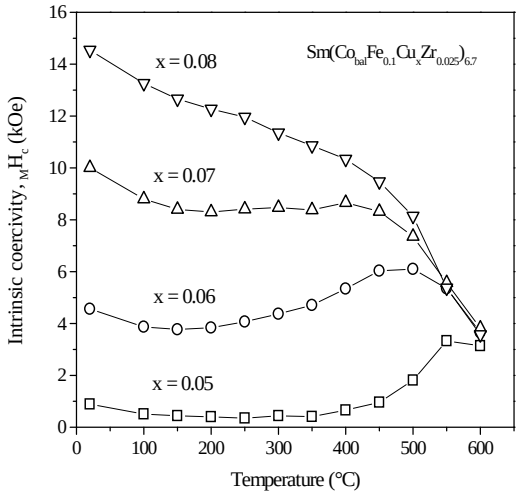


Figure 3-4. Temperature dependence of intrinsic coercivity for $Sm(Co_{bal}Fe_{0.1}Cu_xZr_{0.025})_{6.7}$.

### 3.1.4. Effect of Zr on High Temperature $_MH_c$ of Sm-TM Magnets

Zr has an important effect on the development of coercivity in the $Sm_2(Co,Fe,Cu,Zr)_{17}$ type magnets. It has been observed in this study that Zr is critical in developing high coercivity at both low and high temperatures. It was observed that intrinsic coercivity rapidly increased with increasing Zr and a peak coercivity value was reached at an optimum Zr content. The squareness of the 2nd quadrant demagnetization curve is strongly depended on Zr content in magnet alloys. The knee field rapidly enhances with increasing Zr content.

Effects of other transition metals, such as , Ti, Hf, Nb, V, Ta, Cr, and Ni, on high-temperature coercivity of the $Sm_2(Co,Fe,Cu,Zr)_{17}$ were also investigated. All these elements decreased magnetization. Only Nb demonstrated an effect of slightly enhancing coercivity at high temperatures.

### 3.2. New Sm-Co based high-temperature permanent magnet materials

Above mentioned research on effects of compositions on high temperature performance of the 2:17 type of permanent magnets has resulted in a new series of permanent magnets with significantly improved high-temperature performance. The operating temperature of these magnets has been increased from previous 300°C of conventional high-temperature magnets to as high as 550°C. The $_MH_c$ of these new magnets reached 13 kOe at 400°C (2 to 3 times higher than conventional magnets) and 9 kOe at 500°C (4 to 9 times higher than conventional magnets). The B curves of the new magnets remain linear up to 550°C (250 to 350°C higher than conventional magnets). The temperature coefficients of $_MH_c$ for the new magnets can range from a small negative value (-0.1%/°C), to near zero, or they may even be positive (up to +1.7%/°C). As a comparison, the temperature coefficients of $_MH_c$ for conventional $SmCo_5$, $Sm_2TM_{17}$, and $Nd_2Fe_{14}B$ magnets around room temperature are –0.3%/°C, -0.3%/°C, and –0.9 %/°C, respectively.

Figure 3-5 shows demagnetization curves of $Sm(Co_{bal}Fe_{0.09}Cu_{0.09}Zr_{0.03})_{7.69}$ at 400, 450, and 500°C. This magnet illustrates much higher ${}_MH_c$ and better squareness of demagnetization curves at high temperatures than the conventional 2:17 magnets. Figure 3-6 displays the temperature dependence of ${}_MH_c$ for some newly developed sintered Sm-Co based permanent magnets. For comparison, the temperature dependence of ${}_MH_c$ of a high-coercivity type of conventional 2:17 magnet is also shown as Curve 1 in the figure. It can be seen from Figure 3-6 that the ${}_MH_c$ of the new magnets is much less temperature sensitive in comparison with the conventional 2:17 magnet. At temperatures above 100°C, the ${}_MH_c$ of $Sm(Co_{bal}Fe_{0.09}Cu_{0.09}Zr_{0.03})_{7.69}$ (Curve 2) is higher than that of the conventional 2:17 magnet. At 400°C, the ${}_MH_c$ is three times higher than that of the conventional magnet. Curve 4 has a very flat portion at a quite high coercivity level from 200 to 400°C. From room temperature to 450°C, the ${}_MH_c$ of $Sm(Co_{bal}Fe_{0.09}Cu_{0.09}Zr_{0.025})_{7.14}$ remains almost constant (Curve 5), making its temperature coefficient very close to zero over this wide temperature range. In addition, we observed a complex temperature dependence of ${}_MH_c$ in some newly developed magnets (Curve 6).

The variation of temperature coefficients of ${}_MH_c$ as a function of temperature for the magnets shown in Figure 3-6 is given in Figure 3-7. As a comparison, Figure 3-7 also gives temperature coefficients of ${}_MH_c$ of a typical $SmCo_5$ and a Nd-Fe-B magnet. The temperature coefficient of ${}_MH_c$ demonstrated in Figure 3-7 is defined as

$$\beta = \frac{d({}_M H_c)}{dT} \; X \; \frac{100}{{}_M H_c} \quad (\%/°C). \tag{1}$$

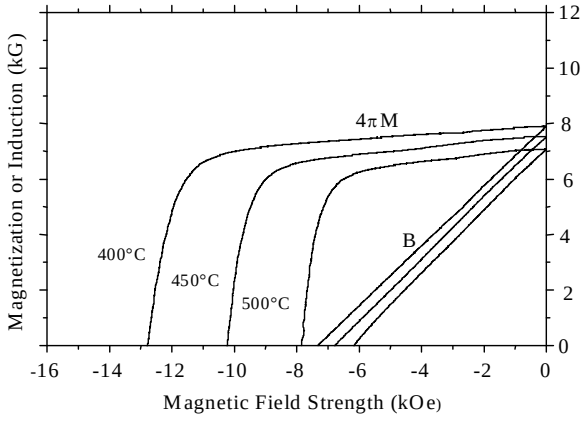


Figure 3-5. Demagnetization curves of $Sm(Co_{bal}Fe_{0.09}Cu_{0.09}Zr_{0.03})_{7.69}$ at 400°C, 450°C, and 500°C.

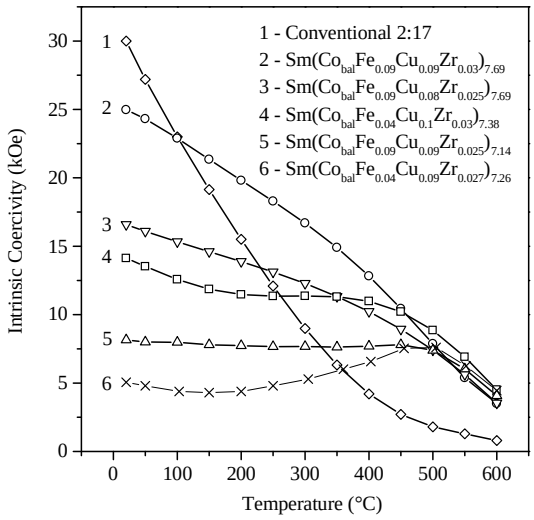


Figure 3-6. Temperature dependence of intrinsic coercivity of various Sm(Co,Fe,Cu,Zr)z magnets.

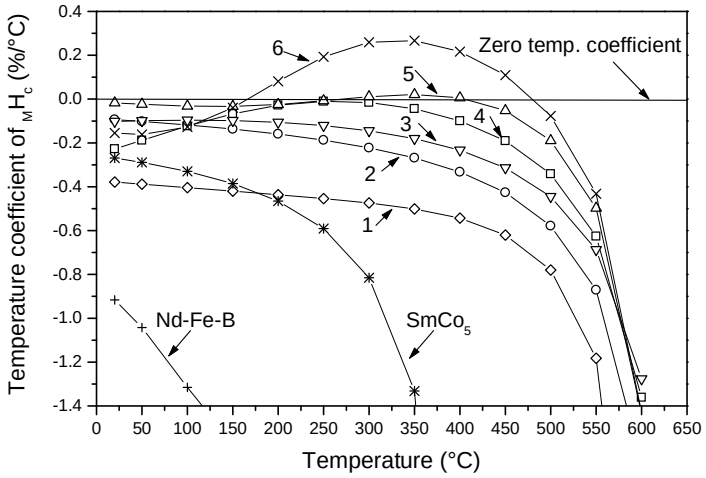


Figure 3-7. Temperature coefficients of various permanent magnets. Numbers (1-6) denote the same magnets as shown in Figure 3-6.

### 3.2 Dynamic Characterizations of New High-Temperature Permanent Magnets

It is important to realize that the typical magnetic characterization is a static characterization. Its results are only meaningful to the static applications in which the operating point of a magnet in the induction demagnetization curve is fixed. Data obtained from a static characterization do not necessarily represent the real capability of a magnet in dynamic applications in which the operating point of the magnet in the induction demagnetization curve is cycled. Examples of dynamic applications are motors, generators, magnetic bearings, and magnetic actuators.

Because these important applications of permanent magnets are dynamic applications, it is of the utmost importance to know the capability of a magnet under dynamic rather than static conditions. Bearing this in mind, we devised two sets of dynamic characterizations. In the first one the magnet specimens were magnetically cycled under an applied demagnetizing field of 0 to $_BH_c$ before their magnetic properties were determined. The first set of characterizations was performed from room temperature to 500°C. The second set of characterizations was carried out at a fixed temperature of 400°C with applied demagnetizing field raging from 0 to 9 kOe. We compared the dynamic magnetic properties of the new magnets with those of the best conventional 2:17 in these two sets of dynamic characterizations. The maximum operating temperature of the magnet specimens used in these dynamic characterizations is 450°C.

Results of the first set of dynamic characterization are summarized in Figure 3-8. It should be noted that at room temperature the conventional 2:17 has higher dynamic $(BH)_{max}$. However, at about 250°C, the dynamic $(BH)_{max}$ of the conventional 2:17 begins to sharply decrease. At 400°C, $(BH)_{max}$ drops to less than 1/20 of the new magnet. Results of the second set of dynamic characterizations are summarized in Figure 3-9. It is obvious that the maximum applied demagnetizing field to which the best conventional 2:17 can be subjected without significant loss of $(BH)_{max}$ was about 2 kOe, while for the new magnet, it is as high as 8 kOe.

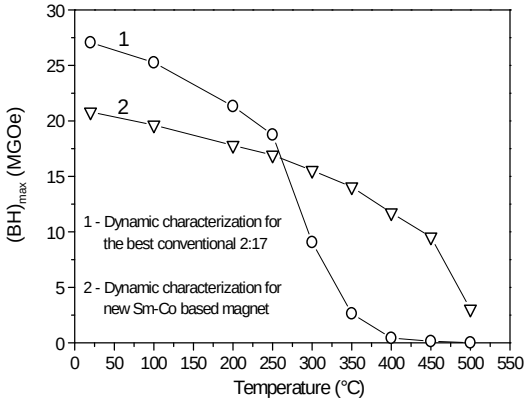


Figure 3-8. A summary of the first set of dynamic characterizations.

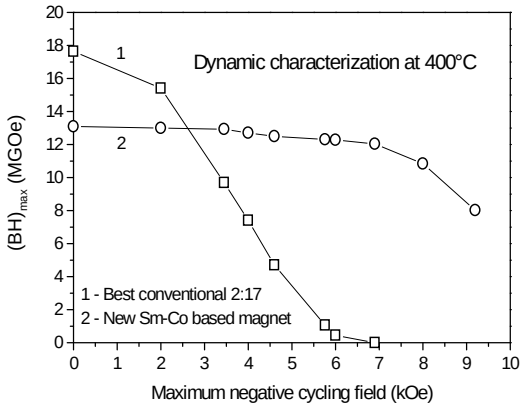


Figeur 3-9. A summary of the second set of dynamic characterizations.

### 3.3 Long-Term Thermal Stability of New High-Temperature Permanent Magnets

A conventional aging experiment was also performed to test the long-term high-temperature stability of the new magnets. Figure 3-10 shows the loss of flux density in the first 100 hours for $Sm(Co_{0.795}Fe_{0.09}Cu_{0.09}Zr_{0.025})_z$, with effective z = 7.26, 7.62, 7.86, and 8.10, in a conventional long-term aging experiment performed at 500°C in air. As comparisons, data for a best conventional high temperature 2:17-28 magnet (room temperature $(BH)_{max}$ = 28 MGOe), a conventional 2:17-30 magnet (room temperature $(BH)_{max}$ = 30 MGOe) are also included in the figure. Figure 3-11 shows the loss of flux density up to 2000 hours for the same magnets. It is obvious from Figure 3-11 that the newly developed magnets display significantly lower losses of flux density than the conventional 2:17 magnets under the same testing condition. The magnet with z = 7.62 gives the best long-term stability. Magnets with the z values lower or higher than 7.62 illustrate relatively larger losses. It is observed that the magnet with z = 7.26 displays the largest loss among the four new magnets though at high temperatures it has higher $_MH_c$ than magnets with z = 7.86 and z = 8.10 (Fig. 3.2???). This is related to the fact that it has low room temperature $_MH_c$.

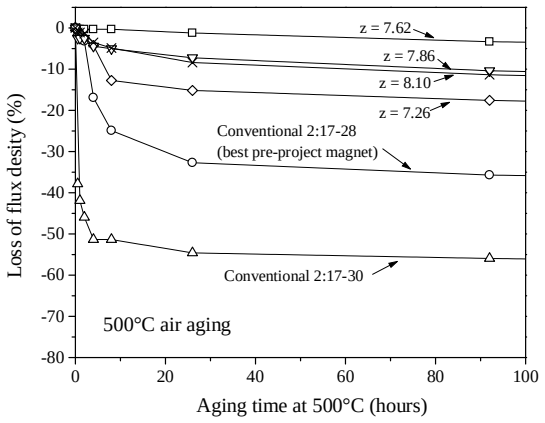


Figure 3-10. Loss of flux density vs. aging time at 500°C for the first 100 hours.

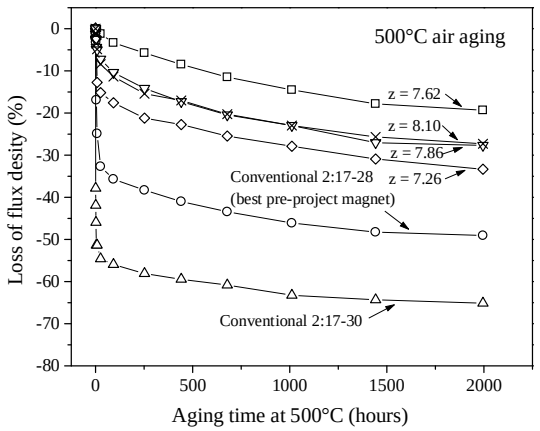


Figure 3-11. Loss of flux density vs. aging time at 500°C up to 2000 hours.

### 3.4 Microstructure and Crystal Structure

Figure 3.12 is an optical micrograph of $Sm(Co_{0.794}Fe_{0.1}Cu_{0.09}Zr_{0.026})_{7.0}$ after aging. The nominal z value of the magnet specimen is 6.46. In other words, the magnet specimen contains very high Sm. Under this condition, it still shows a uniform "one-phase" microstructure. Figure 3-13 is a TEM micrograph of a new high-temperature magnet. It is seen from Figure 3-13 that the cellular structure in the magnet is smaller than that in conventional 2:17 magnets.

Figure 3-14 is the XRD pattern of $Sm(Co_{0.794}Fe_{0.09}Cu_{0.09}Zr_{0.026})_{7.0}$ after solid-solution heat treatment (SSHT). This figure shows that the magnet specimen is of 1:7 hexagonal crystal structure in the SSHT condition. Figure 3-15 is the XRD pattern of the same magnet after aging and in high coercivity condition. The XRD result indicates that the magnet specimen consists of a 2:17 rhombohedral phase and a 1:5 hexagonal phase.

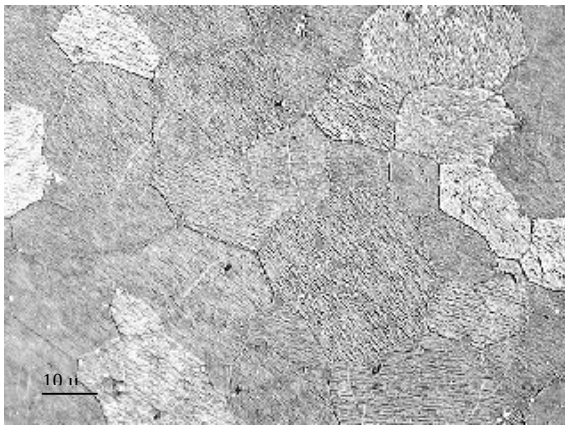


Figure 3.-2. Optical micrograph of $Sm(Co_{0.794}Fe_{0.1}Cu_{0.09}Zr_{0.026})_{7.0}$ (Nominal z = 6.46)

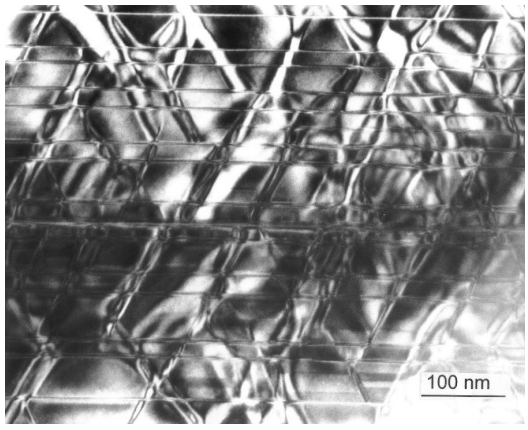


Figure 3-13. TEM micrograph of a new magnet. (Courtesy to Dr. J. Fidler of the University of Vienna, Austria.)

### 3.9 Novel temperature dependence of intrinsic coercivity

Novel temperature dependence of $_MH_c$ was observed in some of newly developed magnets. For example, when heating a magnet of $Sm(Co_{bal}Fe_{0.04}Cu_{0.09}Zr_{0.027})_{7.26}$ it $_MH_c$ first gradually decreases and reaches a minimum at about 150°C as shown in Figure 3-16. With continued heating, the $_MH_c$ of this magnet rapidly increases and forms a maximum at 500°C. The $_MH_c$ of this magnet at 500°C is more than 30% higher than its room temperature value! This abnormal temperature variation of $_MH_c$ also affects its $(BH)_{max}$ as shown in Figure 3-16 Another magnet of $Sm(Co_{0.825}Fe_{0.1}Cu_{0.05}Zr_{0.025})_{7.38}$ displays a maximum $_MH_c$ at 550°C which is nearly four times higher than its room temperature coercivity value as shown in Figure 3-17. It has become aware that similar abnormal temperature dependence of coercivity was observed by Russian researches in 1998 [13,14].

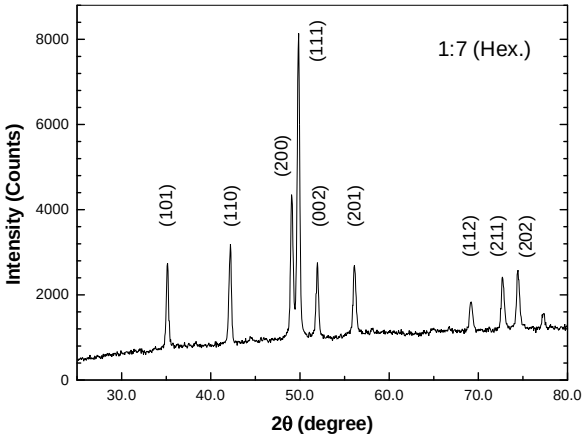


Fig.3. 14. XRD pattern of $Sm(Co_{0.794}Fe_{0.09}Cu_{0.09}Zr_{0.026})_{7.0}$ after solid solution heat treatment.

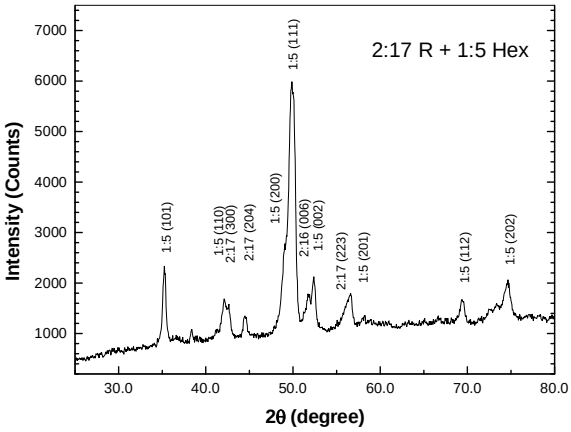


Fig. 3 15. XRD pattern of $Sm(Co_{0.794}Fe_{0.09}Cu_{0.09}Zr_{0.026})_{7.0}$ after aging.

The complex temperature dependence of coercivity can be explained by taking into account the effects of temperature not only on the basic magnetic parameters, such as magneto-crystalline anisotropy, but also on the thermal activation of domain walls. It is believed that the energy, necessary for domain walls to overcome the energy barrier between the 1:5 cell boundary phase and the 2:17 cell phase, can be acquired not only from the applied magnetic field, but also from thermal energy $k_BT$. In other words, the domain wall motion in the 2:17 magnets can be treated as a thermal activation process. This consideration gives rise to an expression of

$$_MH_c = c\ exp(\Delta E(T)/k_BT), \qquad (2)$$

where $c$ is a constant, $k_B$ is the Boltzmann constant, and $\Delta E(T)$ is the energy barrier between the cell boundary phase and the cell phase.

This new pinning-thermal activation model of coercivity satisfactorily explains abnormal temperature dependence of coercivity as well as "normal" temperature dependence of coercivity in conventional magnets. This concept may apply to all ferromagnetic materials in which domain wall motion is involved during magnetization and demagnetization. For example, in soft magnetic materials the coercivity is determined by the maximum resistance to the domain wall motion. This resistance can be caused by any crystal imperfection, including grain boundaries, inclusions, precipitates, strain, and stress. The energy necessary for the domain walls to overcome an energy barrier $\Delta E(T)$ can be obtained not only from magnetic energy, but also from thermal energy $k_BT$. In general, the susceptibility of a soft magnetic material may be expressed as

$$\kappa \propto exp(k_BT / \Delta E(T)). \qquad (3)$$

However, since the domain walls in soft magnetic materials are quite thick resulting from the low magnetocrystalline anisotropy, thermal activation of domain walls in soft magnetic materials is probably more difficult than in magnetic materials with high crystalline anisotropy.

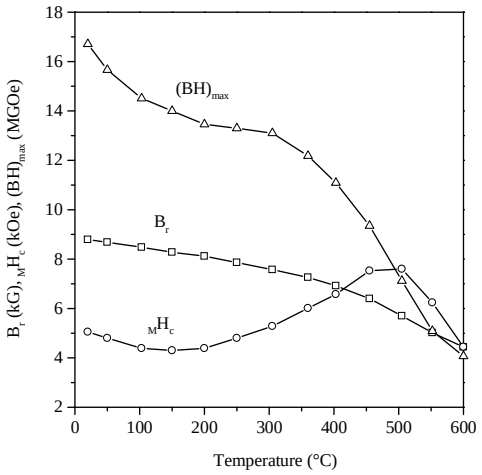


Figure 3.16. Temperature dependence of magnetic properties of $Sm(Co_{bal}Fe_{0.04}Cu_{0.09}Zr_{0.027})_{7.26}$

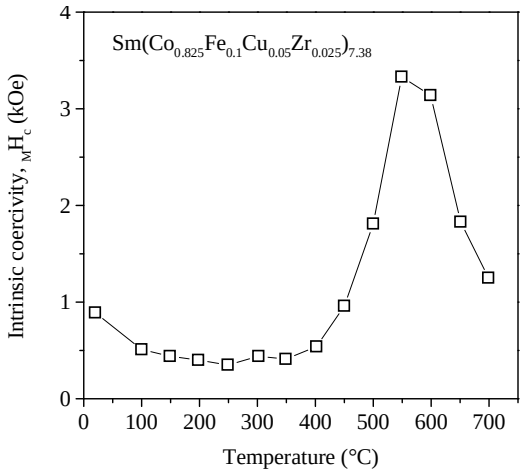


Figure 3.17. Temperature dependence of intrinsic coercivity of $Sm(Co_{0.825}Fe_{0.1}Cu_{0.05}Zr_{0.025})_{7.38}$ magnet.

## REFERENCES

[1] K.J. Strnat, IEEE Trans. Magn. 23 (1987), 2094.

[2] A.E. Ray, J. Appl. Phys. 55 (1984), 2094.

[3] A.E. Ray, IEEE Trans. Magn. 20 (1984), 1614.

[4] A.E. Ray, J. Appl. Phys. 67 (1990), 4972.

[5] S. Liu, H.F. Mildrum, and K.J. Strnat, J. Appl. Phys. 53 (1982), 2383.

[6] S. Liu and A.E. Ray, IEEE Trans. Magn. 25 (1989), 3785.

[7] S. Liu and E. P. Hoffman, IEEE Trans. Magn. 32 (1996), 5091.

[8] B. M. Ma, Y. L. Liang, J. Patel, D. Scott, and C. O. Bounds, IEEE Trans. Magn. 32, (1996), 4377.

[9] C. H. Chen, M. S. Walmer, M. H. Walmer, S. Liu, E. Kuhl, and G. Simon, J. Appl. Phys. 83 (1998), 6706.

[10] A. Kim, J. Appl. Phys. 83 (1998), 6715.

[11] J. F. Liu, Y. Zhang, Y. Ding, D. Dimitrov, and G. C. Hadjipanayis, Proc. 15th Intl. Workshop on REPM, (1998), 607.

[12] Marlin S. Walmer, Christina H. Chen, Michael H. Walmer, Sam Liu, and G. Edward Kuhl, IEEE Trans. Magn. 36 (2000), to be published.

[13] A.G. Popov, A.V. Korolev, and N.N. Shchegoleva, Phys. Met. Metall. 69 (1990), 100.

[14] A.G. Popov, V.S. Gaviko, L.M. Magat, and G.V. Ivanova, Phys. Met Metall. 70 (1990), 18.